

Density dependence of the *s*-wave repulsion in pionic atoms

E. Friedman

Racah Institute of Physics, The Hebrew University, Jerusalem 91904, Israel

Abstract

Several mechanisms of density dependence of the *s*-wave repulsion in pionic atoms, beyond the conventional model, are tested by parameter fits to a large (106 points) set of data from ^{16}O to ^{238}U , including ‘deeply bound’ states in ^{205}Pb . Special attention is paid to the proper choice of nuclear density distributions. A density-dependent isovector scattering amplitude suggested recently by Weise to result from a density dependence of the pion decay constant is introduced and found to account for most of the so-called anomalous repulsion. The presence of such an effect might indicate partial chiral symmetry restoration in dense matter. The anomalous repulsion is fully accounted for when an additional relativistic impulse approximation term is included in the potential.

PACS: 13.75-n; 13.75.Gx; 25.80Hp

Keywords: pionic atoms, *s*-wave repulsion, chiral restoration

Corresponding author: E. Friedman,
Tel: +972 2 658 4667, FAX: +972 2 658 6347,
E mail: elifried@vms.huji.ac.il

May 21, 2019

I. INTRODUCTION

Strong interaction effects in pionic atoms have been studied for several decades both experimentally and theoretically [1]. A theoretically-motivated phenomenological pion-nucleus potential [2] has been quite successful in reproducing the experimental values of strong interaction level shifts and widths throughout the periodic table. This potential has a local part which is effective over the whole of the nuclear volume and a p -wave part which is effective only in the surface region of the nucleus. Both components have terms linear in the nuclear densities which are closely related to the free pion-nucleon interaction, and quadratic (complex) terms which originate from pion absorption on pairs of nucleons. The latter are mostly determined empirically from fits to data whereas the former, although determined empirically, may also be calculated from the pion-nucleon interaction in free space. The p -wave component of the potential turns out to be fairly well understood, but the s -wave part of the potential had turned out too repulsive compared with expectations [3,4].

The renewed interest in pionic atoms in general and in the s -wave part of the potential in particular stems from two recent developments. The first is the experimental observation of ‘deeply bound’ pionic atom states in the $(d, {}^3\text{He})$ reaction [5,6] whose existence was predicted a decade earlier [7–9]. The second is the very accurate measurement of the shift and width of the $1s$ level in pionic hydrogen [10] which leads to precise values of the s -wave scattering lengths.

Very recent attempts to explain the above mentioned s -wave repulsion in terms of a density dependence of the pion decay constant were made by Weise and Kaiser [11,12]. The proposed mechanism was implemented in fits to a large set of pionic atom data [13] and indeed found to remove most of the ‘anomaly’ in the s -wave term. A relativistic impulse approximation (RIA) term that was proposed earlier following Birbrair [14–18] was also shown [17,13] to remove part of the anomaly. Combining the two effects [13] removed the anomaly completely.

The present work is an extension of Ref. [13] in several respects. First, the data base of the present work contains 106 data points compared to 60 points in the earlier work. The additional data are mostly from the work of the Amsterdam group (see [19] and references therein) which includes several sequences of isotopes, of particular importance in the present context where most of the effect is due to an isovector term (see below). The second difference compared to the earlier work is in the nuclear density distributions, where in addition to ‘macroscopic’ densities [1] we have used ‘single particle’ densities constrained by results of relativistic mean field calculations. The third difference is that in the present work more flexibility was allowed in the RIA model and in the χ^2 fits. The general context of the present work is the use of several models for the pion-nucleus interaction, each resulting in a well-defined functional of the local nuclear densities. Fits to a large set of experimental data provide the parameters of these various functionals.

The paper is organized as follows. Section II describes the pion-nucleus potential, including discussion of the nucleon densities. Section III summarizes the data base and the fit procedures. The results are given in Section IV and Section V is a summary.

II. THEORETICAL BACKGROUND

The interaction of pions at threshold with the nucleus is described by the Klein-Gordon (KG) equation of the form:

$$[\nabla^2 - 2\mu(B + V_{\text{opt}} + V_c) + (V_c + B)^2] \psi = 0 \quad (\hbar = c = 1) \quad (1)$$

where μ is the pion-nucleus reduced mass, B is the complex binding energy and V_c is the finite-size Coulomb interaction of the pion with the nucleus, including vacuum-polarization terms. Equation (1) assumes that the strong interaction potential V_{opt} behaves as a Lorentz scalar. The potential is usually taken as suggested by Kisslinger [20] and modified by Ericson and Ericson [2] to include absorption of pions on pairs of nucleons. The form used in the present work is

$$2\mu V_{\text{opt}}(r) = q(r) + \vec{\nabla} \cdot \alpha(r) \vec{\nabla} \quad (2)$$

with

$$\begin{aligned} q(r) = & -4\pi(1 + \frac{\mu}{M})\{\bar{b}_0(r)[\rho_n(r) + \rho_p(r)] + b_1[\rho_n(r) - \rho_p(r)]\} \\ & -4\pi(1 + \frac{\mu}{2M})4B_0\rho_n(r)\rho_p(r), \end{aligned} \quad (3)$$

$$\alpha(r) = \frac{\alpha_1(r)}{1 + \frac{1}{3}\xi\alpha_1(r)} + \alpha_2(r), \quad (4)$$

where

$$\alpha_1(r) = 4\pi(1 + \frac{\mu}{M})^{-1}\{c_0[\rho_n(r) + \rho_p(r)] + c_1[\rho_n(r) - \rho_p(r)]\}, \quad (5)$$

$$\alpha_2(r) = 4\pi(1 + \frac{\mu}{2M})^{-1}4C_0\rho_n(r)\rho_p(r). \quad (6)$$

In these expressions ρ_n and ρ_p are the neutron and proton density distributions normalized to the number of neutrons N and number of protons Z , respectively, and M is the mass of the nucleon. In this potential $q(r)$ is referred to as the s -wave potential term and $\alpha(r)$ is referred to as the p -wave potential term. The function $\bar{b}_0(r)$ is given in terms of the *local* Fermi momentum k_F

$$\bar{b}_0(r) = b_0 - \frac{3}{2\pi}(b_0^2 + 2b_1^2)k_F(r), \quad (7)$$

where b_0 and b_1 are minus the pion-nucleon isoscalar and isovector scattering lengths, respectively. The coefficients c_0 and c_1 are the pion-nucleon isoscalar and isovector p -wave scattering volumes, respectively. The parameters B_0 and C_0 represent s -wave and p -wave absorptions, respectively, and as such they have imaginary parts. Dispersive real parts are found to play an important role in pionic atom potentials. The parameter ξ is the usual Ericson-Ericson Lorentz-Lorenz coefficient (EELL) [2]. The terms with $4\rho_n\rho_p$ were originally

written as $(\rho_n + \rho_p)^2$ (see Ref. [2]), but the results hardly depend on which form is used. An additional relatively small term, known as the ‘angle-transformation’ term (see Eq.(24) of [1]), is also included.

The potential as described above had been used extensively to analyze pionic atom data [1,19]. It will be referred to in the following as the conventional potential (C). Very good fits to the data are obtained with this potential but the combined repulsion due to the resulting values of the parameters b_1 and $\text{Re}B_0$ is about twice as large as is expected from the very well known values of the free pion-nucleon scattering lengths [10] and from the well-determined parameter $\text{Im}B_0$ [1,19]. For that reason the *s*-wave interaction in the nuclear medium continued to be a topic of interest. Very recently Weise [11] showed that if the pion decay constant in nuclear matter f_π^* is given, in leading order, as a function of the local density ρ

$$f_\pi^{*2} = f_\pi^2 - \frac{\sigma_N}{m_\pi^2} \rho \quad (8)$$

where f_π is the decay constant of the pion in free space and σ_N is the pion-nucleon sigma term, then the *s*-wave scattering amplitude becomes a function of the local density as follows

$$b_1(\rho) = \frac{b_1(0)}{1 - 2.3\rho} \quad (9)$$

for $\sigma_N=50$ MeV and with ρ in units of fm^{-3} . The parameter $b_1(0)$ refers to the experimental free pion-nucleon interaction at threshold [10]. Introducing this function of the local density into the above potential, in Eq.(3) and (7), leads to the ‘W’ potential of Ref. [13]. If $b_1(0)$ is taken as the first order chiral perturbation result of Weinberg, then a third order correction of about 15% brings it in line with the experimental value of [10]. In that case there is an additional density dependence in Eq.(9) which, however, does not affect the results for pionic atoms beyond what is obtained when Eq.(9) is used with the empirical pion-nucleon value. We therefore refer to the experimental free pion-nucleon value throughout, denoting this potential by ‘W’.

Among several previous attempts to account for the anomalous *s*-wave repulsion a relativistic impulse approximation approach showed [14–18] that a specific version of the RIA was able to provide a significant part of the anomalous repulsion through the modification of the *nucleon* mass in the nuclear medium. This version of the RIA was considered as an additional option in [13] and is included in the present work, using the following parameterization [16]

$$\frac{M(\rho)}{M(0)} = \frac{1}{1 + a\rho}. \quad (10)$$

With $a=2.7 \text{ fm}^3$, we find $M(\rho)/M(0) = 0.7$ for the nucleon mass ratio at normal nuclear density. With $a=1.56 \text{ fm}^3$ this ratio is 0.8. Both values have been used in the present work.

The nuclear densities ρ_p and ρ_n are essential ingredients of the pion-nucleus potential, and have been discussed at some length in [1]. Two questions are relevant in connection with nuclear densities: (i) the model used to generate the densities and (ii) the radial extent of the neutron densities. The root mean square (rms) radii of the proton densities are obtained from the experimentally determined charge distributions [21] by unfolding the finite size of

the proton. In the present work we have used both the macroscopic (MAC) densities and the single particle (SP) densities discussed in [1]. In previous analyses [19,1,13] the rms radii of the neutron densities (r_n) were assumed equal to the corresponding rms radii for the protons (r_p) in the case of light ($N = Z$) nuclei, and were taken to be slightly larger than the corresponding radii for the protons for $N > Z$ nuclei. Here we have used those previous values and in addition we used rms radii for the neutron densities as obtained from recent relativistic mean field (RMF) predictions [22] for the *differences* $r_n - r_p$. The sensitivity of the results to the precise values of r_n is small. However, attempting to use neutron densities with $r_n = r_p$ resulted in major deterioration in the quality of fits to the data.

Finally we remark that the strong interaction shifts are always taken relative to the corresponding electromagnetic values calculated from the *finite size* charge of the nucleus and including vacuum polarization terms. This is the conventional definition and actually the only one meaningful for $1s$ states in heavy nuclei ($Z > 137/2$).

III. DATA BASE AND FIT PROCEDURES

The data base for the present work of 106 data points was made by adding 46 points to the 60 points used in Ref. [13]. Those 60 points were the 54 points of Ref. [1] to which were added the shift and width of the $4f$ level in ^{208}Pb [19] and the recently obtained results [23,24] for the ‘deeply bound’ $1s$ and $2p$ states in pionic atoms of ^{205}Pb . In the case of the deeply bound states the shifts, relative to the finite size and vacuum polarization values discussed in the previous section, were simply obtained from the experimental binding energies [23,24]. The shift of the $4f$ level as well as the 23 additional shifts [19] were transformed to our normal basis of the finite size plus vacuum polarization reference using the parameters of the charge distributions listed in Ref. [19].

The parameters of the pion-nucleus potential were varied in χ^2 minimization, where χ^2 was defined in the usual way. With so many data points it was possible to vary simultaneously all 9 parameters of the potential, but obviously some were determined better than the others and also correlations exist between some parameters. The final results were therefore obtained by usually varying only 6 or 7 parameters, as is discussed in the next section. All fits were repeated for the four types of density distributions mentioned in the previous section, namely for two sets of MAC densities and for two sets of SP densities. The whole process was repeated six times, using the conventional (C) potential, the Weise (W) potential, two RIA potentials with different values of the parameter a (Eq.(10)) and two potentials where both the RIA and the W mechanisms were included.

IV. RESULTS

Starting with the conventional potential it was easy to obtain fits with χ^2/F , the χ^2 per degree of freedom, of about 1.9. This represents very good fits to pionic atom data from ^{16}O to ^{238}U , covering atomic states from $1s$ to $4f$. The fits to the deeply bound $1s$ and $2p$ states in ^{205}Pb were better than the average. The results of these large scale fits were in general agreement with previous works [1,19]. Of particular importance in the present context is the very weak coupling found between the s -wave part of the potential which is effective

over the nuclear volume and the p -wave part of the potential which is effective only in the surface region. The EELL parameter ξ was not well determined and a broad minimum was obtained for values around 2 or larger. However, the scattering volume parameters c_0 and c_1 turned out to be close to the free pion-nucleon values only when ξ was close to 1. Using the property of the p -wave term of being effective only near the nuclear surface, we chose to keep the value of ξ fixed at 1. The parameter c_1 was always found to be consistent with the free pion-nucleon value and consequently it was kept fixed at that value in the final fits. The parameter c_0 too was kept fixed in part of the fits, although marginal improvements in the fits could be obtained when it was varied slightly. Each fit was repeated 8 times: for the two sets of rms radii for neutron density distributions, for the MAC and SP models used to generate the density distributions and for c_0 fixed or variable. All the fits for the conventional (C) potential produced almost the same values of χ^2/F which makes it impossible to prefer any one of them on the basis of quality of fit. Introducing additional absorption terms proportional to ρ_p^2 [19] produced insignificant improvements. One difference compared to the earlier analysis [13] was that $\text{Re}C_0$ was not consistent with zero and therefore it was varied in all fits.

The other five potentials, each with additional dependence on the nuclear density relative to the conventional potential, were used in fits to the data in much the same way. Typical results are summarized in Table I. In this table the Weise model (Eq.(9)) is labelled by W and the two RIA models with $a=2.7$ and $a=1.56 \text{ fm}^3$ (Eq.(10)) are labelled by B1 and B2, respectively. The rows WB1 and WB2 are for fits when the Weise and the RIA models were combined. It is seen from the table that the quality of the fits is essentially the same for all the potentials and therefore other criteria must be applied in order to prefer one potential or the other.

The anomalous repulsion in the s -wave part of the potential can be seen in Table I through values of b_1 and $\text{Re}B_0$. For the C potential the former is significantly more repulsive than the free pion-nucleon value and the latter, which is the dispersive part of the absorptive term $\text{Im}B_0$, is repulsive with a magnitude 3-4 times larger than the absorption. This is quite unacceptable as various theoretical approaches [4,25,26] suggest that the real part must have about the same magnitude as the imaginary part. The other rows in the table show various degrees of reduced repulsion in b_1 and in $\text{Re}B_0$. This is achieved through the density dependence of b_1 in the Weise model which makes b_1 progressively more repulsive with increasing nuclear density and through the repulsion generated by the RIA term. In both cases the phenomenological repulsion required by the data is obtained while keeping b_1 closer to the free nucleon value and keeping $\text{Re}B_0$ closer to expectations.

Figures 1 and 2 show the values of b_0 , b_1 and $\text{Re}B_0$ for all the 48 different fits. The six groups of eight points each are according to the potential (see Table I), the type of nuclear density used and for both fixed c_0 and variable c_0 . Figure 1 includes, between horizontal dashed lines, the experimental values of the free pion-nucleon b_0 and b_1 parameters. The horizontal dashed lines in Figure 2 show the range of expected values of $\text{Re}B_0$ between $-\text{Im}B_0$ and $\text{Im}B_0$. Within each potential one can see a fairly small dependence on details such as type of density and whether c_0 was varied or not. The anomalous repulsion is clearly seen for the conventional potential. It essentially disappears for potential WB2.

Figure 3 shows values of χ for all the data points, for fits based on the C and W potentials with MAC densities. It illustrates that there are no systematic differences between the

different potentials from the point of view of fits to the data. Very similar results are obtained when different nuclear densities are used. It seems that whatever systematics is observed in Fig. 3 it is peculiar to the targets and not to differences between the models used here. Obviously it could indicate deficiencies in the models.

Another topic of interest is the way the real s -wave potential varies from the nuclear surface towards the nuclear interior. As an example Fig. 4 shows the real part of the π^- ^{208}Pb potential for the six models of the present work, based on MAC densities. All six potentials produce almost identical fits to the data (see Table I) and indeed they are almost identical throughout the nucleus. Note that the potentials do *not* follow the nuclear density distribution because of the various non-linear terms. The almost unique potential all over the nucleus is a result of the featureless shape of the MAC densities. Figure 5 shows, again for ^{208}Pb , the six potentials this time based on SP densities. The C potential for MAC densities is also included as a dashed line. Here we see that all the potentials essentially agree in the surface region near 6.2 fm, which presumably is the region best determined by the data. The potential at that point is about 25 MeV whereas the point where the density is half of the central density (shown on the figures) is at 6.9 fm and the potential there is about 11.8 MeV. The potentials due to the various models, based on the SP densities, differ in the interior because these models extrapolate differently into the nuclear interior due to the structure of the densities and the variety of non linear effects. It is probably safe to conclude that the real potential in the nuclear interior is close to 30-35 MeV, in contrast to the value of 20 MeV found by Yamazaki et al. [27] but in reasonable agreement with the value of 28 ± 3 MeV of Friedman and Gal [28].

V. SUMMARY AND CONCLUSIONS

The prime motivation behind the present work was the recent suggestion [11,12] that the anomalous s -wave repulsion of pions in nuclear matter has its origins in a density dependence of the pion decay constant which reflects the change of QCD vacuum structure in dense matter. The consequences for pionic atoms are evident then through the isovector parameter b_1 of the potential, which is quite important because of the extremely small value of the isoscalar parameter b_0 . The density dependence of the pion decay constant (Eq.(8)) leads to an additional well-defined density dependence in the pion-nucleus potential which can be tested by fits to pionic atom data. The idea was to check the consequences of prescription (8) by applying it to modern and extensive pionic atom data. Possible modifications of B_0 have not been considered because we treat this parameter all along as purely phenomenological without any experimental or theoretical reference values, except for the expectation that $|\text{Re}B_0|$ cannot exceed much the value of $\text{Im}B_0$. Also included was a RIA term, which was shown [17] to explain part of the repulsion, although this term is not unique. A very broad data base had been used and extra care was taken in choosing the nuclear densities which are essential ingredients of the potential. Radii of neutron distributions were varied slightly, and were constrained by recent RMF calculations. If one assumes that radii of neutron density distributions are equal to the corresponding radii for proton distributions, then the fits become totally unacceptable.

The results of the present work show that all the potentials produce rather equivalent fits to the data, displaying small sensitivity to the type of potential, to the type of density or to

the precise values of the rms radii of the neutron distributions. The differences between the various potentials are mostly in the value of b_1 and how close it is to the free pion-nucleon value. The prescription Eq.(9) removes most of the ‘anomaly’ and when an RIA term is also included then the parameters b_0 , b_1 and $\text{Re}B_0$ have most acceptable values. These conclusions provide support to the validity of the correction suggested by Weise [11] to the conventional pion-nucleus interaction.

I wish to acknowledge many stimulating discussions with A. Gal.

This research was partially supported by the Israel Science Foundation.

REFERENCES

- [1] For a recent review see C.J. Batty, E. Friedman, A. Gal, *Phys. Rep.* 287 (1997) 385.
- [2] M. Ericson, T.E.O. Ericson, *Ann. Phys. [NY]* 36 (1966) 323.
- [3] J.G.J. Olivier, M. Thies, J.H. Koch, *Nucl. Phys. A* 429 (1984) 425.
- [4] E. Oset, C. García-Recio, J. Nieves, *Nucl. Phys. A* 584 (1995) 653.
- [5] T. Yamazaki, R.S. Hayano, K. Itahashi, K. Oyama, A. Gillitzer, H. Gilg, M. Knüller, M. Münch, P. Kienle, W. Schott, H. Geissel, N. Iwasa and G. Münzenberg, *Z. Phys. A* 355 (1996) 219.
- [6] H. Gilg, A. Gillitzer, M. Knüller, M. Münch, W. Schott, P. Kienle, K. Itahashi, K. Oyama, R.S. Hayano, H. Geissel, N. Iwasa, G. Münzenberg, T. Yamazaki, *Phys. Rev. C* 62 (2000) 025201.
- [7] E. Friedman and G. Soff, *J. Phys. G: Nucl. Phys.* 11 (1985) L37.
- [8] H. Toki and T. Yamazaki, *Phys. Lett.* B213 (1988) 129.
- [9] H. Toki, S. Hirenzaki, T. Yamazaki and R.S. Hayano, *Nucl. Phys. A* 501 (1989) 653.
- [10] H.-Ch. Schröder, A. Badertcher, P.F.A. Goudsmit, M. Janousch, H.J. Leisi, E. Matsinos, D. Sigg, Z.G. Zhao, D. Chatellard, J.-P. Egger, K. Gabathuler, P. Hauser, L.M. Simons, A.J. Rusi El Hassani, *Eur. Phys. J C* 21 (2001) 473.
- [11] W. Weise, *Nucl. Phys. A* 690 (2001) 98.
- [12] N. Kaiser, W. Weise, *Phys. Lett. B* 512 (2001) 283.
- [13] E. Friedman, *Phys. Lett. B* 524 (2002) 87.
- [14] B.L. Birbrair, V.N. Fomenko, A.B. Gridnev, Yu.A. Kalashnikov, *J. Phys. G: Nucl. Phys.* 9 (1983) 1473; 11 (1985) 471.
- [15] P.F.A. Goudsmit, H.J. Leisi, E. Matsinos, *Phys. Lett. B* 271 (1991) 290.
- [16] B.L. Birbrair, A.B. Gridnev, *Nucl. Phys. A* 528 (1991) 647.
- [17] A. Gal, B.K. Jennings, E. Friedman, *Phys. Lett. B* 281 (1992) 11.
- [18] B.L. Birbrair, A.B. Gridnev, L.P. Lapina, A.A. Petrunin, A.I. Smirnov, *Nucl. Phys. A* 547 (1992) 645.
- [19] Results are summarized in J. Konijn, C.T.A.M. de Laat, A. Taal and J.H. Koch, *Nucl. Phys. A* 519 (1990) 773.
- [20] L.S. Kisslinger, *Phys. Rev.* 98 (1955) 761.
- [21] H. de Vries, C.W. de Jager and C. de Vries, *At. Data Nucl. Data Tables* 36 (1987) 495.
- [22] G.A. Lalazissis, S. Raman, P. Ring, *At. Data Nucl. Data Tables* 71 (1999) 1.
- [23] A. Gillitzer, *Proc. Int. Workshop XXIX on Gross Properties of Nuclei and Nuclear Excitations*, Hirschegg, Austria, Jan 14-20, 2001, p. 56.
- [24] H. Geissel, H. Gilg, A. Gillitzer, R.S. Hayano, S. Hirenzaki, K. Itahashi, M. Iwasaki, P. Kienle, M. Münch, G. Münzenberg, W. Schott, K. Suzuki, D. Tomono, H. Weick, T. Yamazaki, T. Yoneyama, *Phys. Rev. Lett.* 12 (2002) 122301.
- [25] C.M. Ko and D.O. Riska, *Nucl. Phys. A* 312 (1978) 217.
- [26] L.L. Salcedo, K. Holinde, E. Oset and C. Schütz, *Phys. Lett.* B353 (1995) 1.
- [27] T. Yamazaki, R.S. Hayano, K. Itahashi, K. Oyama, A. Gillitzer, H. Gilg, M. Knüller, M. Münch, P. Kienle, W. Schott, W. Weise, H. Geissel, N. Iwasa, G. Münzenberg, S. Hirenzaki, H. Toki, *Phys. Lett. B* 418 (1998) 246.
- [28] E. Friedman, A. Gal, *Phys. Lett. B* 432 (1998) 235.

TABLES

TABLE I. Parameter values from fits to 106 pionic atom data points. Other p -wave parameters were held fixed at $c_0=0.22m_\pi^{-3}$, $c_1=0.18m_\pi^{-3}$ and $\xi=1$. The free pion-nucleon values [10] are $b_0 = -0.0001^{+0.0009}_{-0.0021}m_\pi^{-1}$ and $b_1 = -0.0885^{+0.0010}_{-0.0021}m_\pi^{-1}$

potl.	χ^2/F	$b_0 (m_\pi^{-1})$	$b_1 (m_\pi^{-1})$	$\text{Re}B_0 (m_\pi^{-4})$	$\text{Im}B_0(m_\pi^{-4})$	$\text{Re}C_0 (m_\pi^{-6})$	$\text{Im}C_0(m_\pi^{-6})$
C	1.94	0.030 ± 0.010	-0.113 ± 0.004	-0.21 ± 0.04	0.055 ± 0.002	-0.029 ± 0.009	0.064 ± 0.004
W	1.93	0.018 ± 0.010	-0.095 ± 0.003	-0.14 ± 0.05	0.054 ± 0.002	-0.026 ± 0.009	0.063 ± 0.004
B1	1.95	0.016 ± 0.010	-0.102 ± 0.004	-0.06 ± 0.05	0.054 ± 0.002	-0.026 ± 0.009	0.064 ± 0.004
B2	1.94	0.022 ± 0.008	-0.107 ± 0.004	-0.12 ± 0.03	0.054 ± 0.002	-0.028 ± 0.008	0.064 ± 0.003
WB1	2.01	0.006 ± 0.010	-0.086 ± 0.003	0.00 ± 0.05	0.053 ± 0.002	-0.024 ± 0.009	0.063 ± 0.003
WB2	1.94	0.011 ± 0.010	-0.090 ± 0.003	-0.06 ± 0.04	0.054 ± 0.002	-0.025 ± 0.009	0.063 ± 0.003

FIGURES

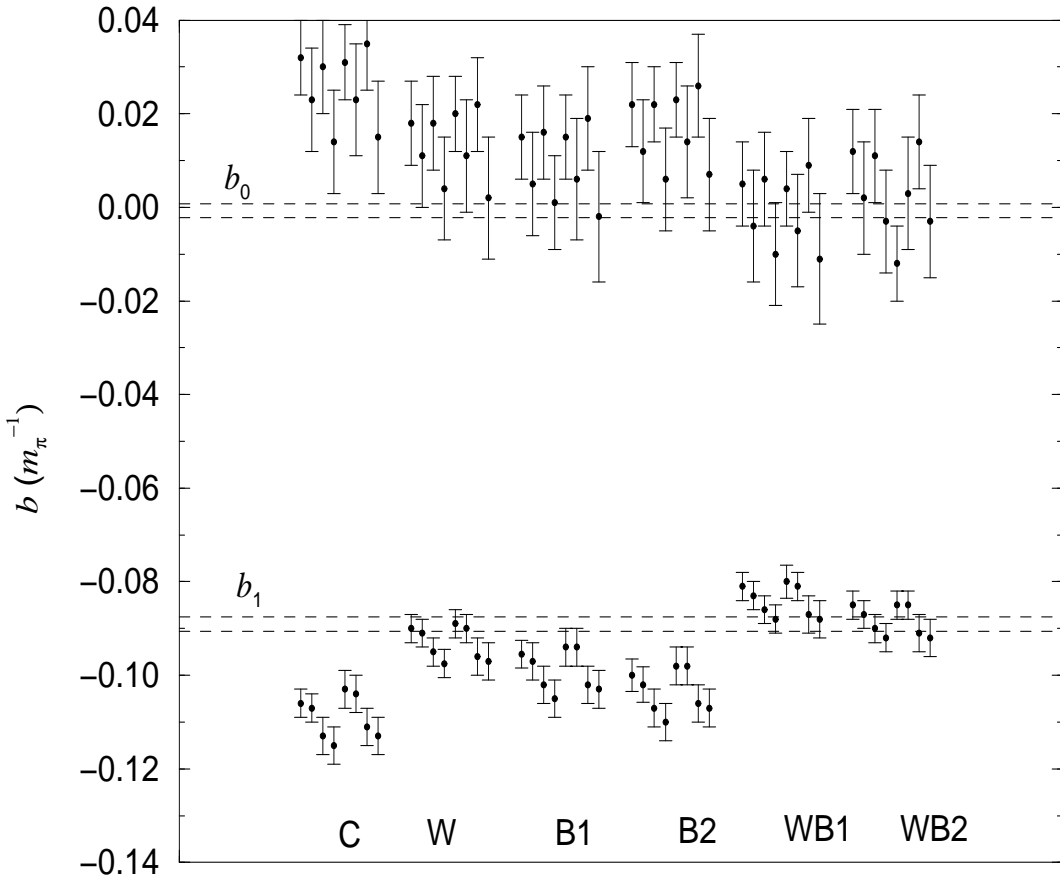


FIG. 1. Values of b_0 and b_1 obtained from fits to pionic atom data for the six potentials indicated and the various densities and fit procedures (see text). The horizontal bands indicate the experimental values for the free pion-nucleon interaction [10].

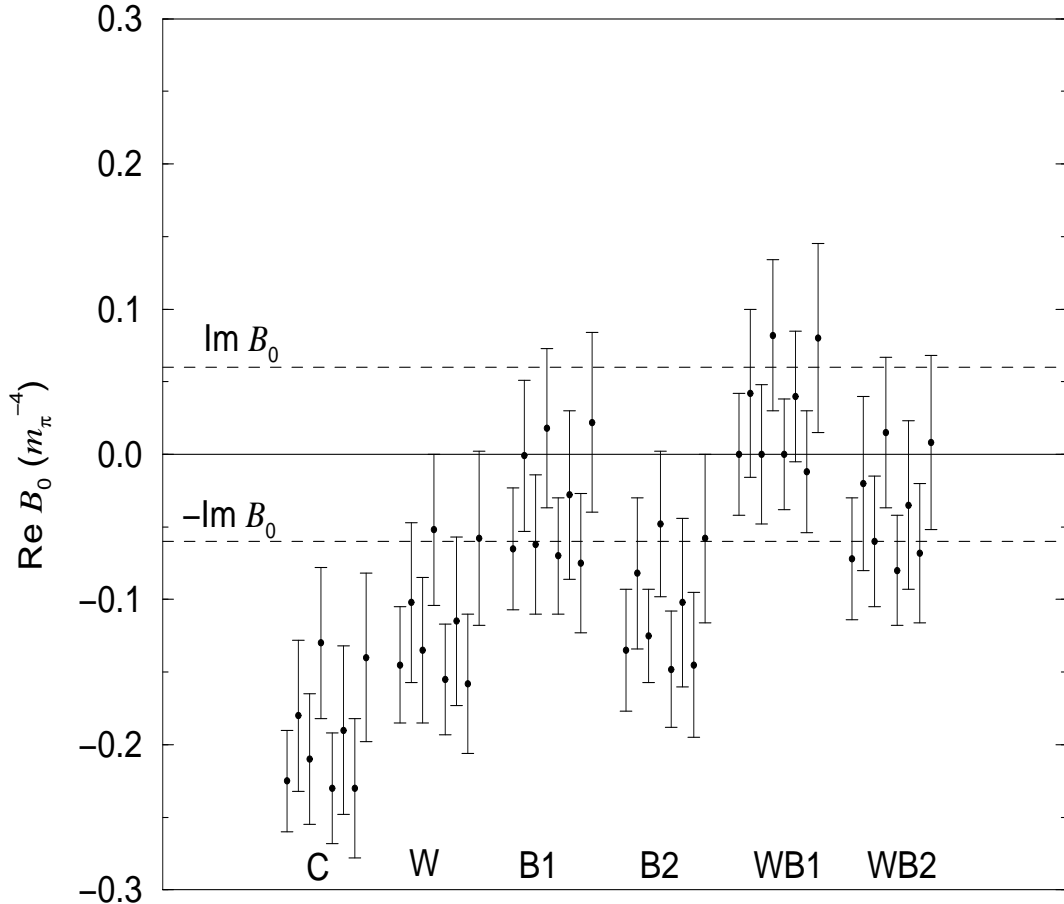


FIG. 2. Values of $\text{Re} B_0$ obtained from fits to pionic atom data for the six potentials indicated and the various densities and fit procedures (see text). The horizontal bands indicate the theoretically expected range of values.

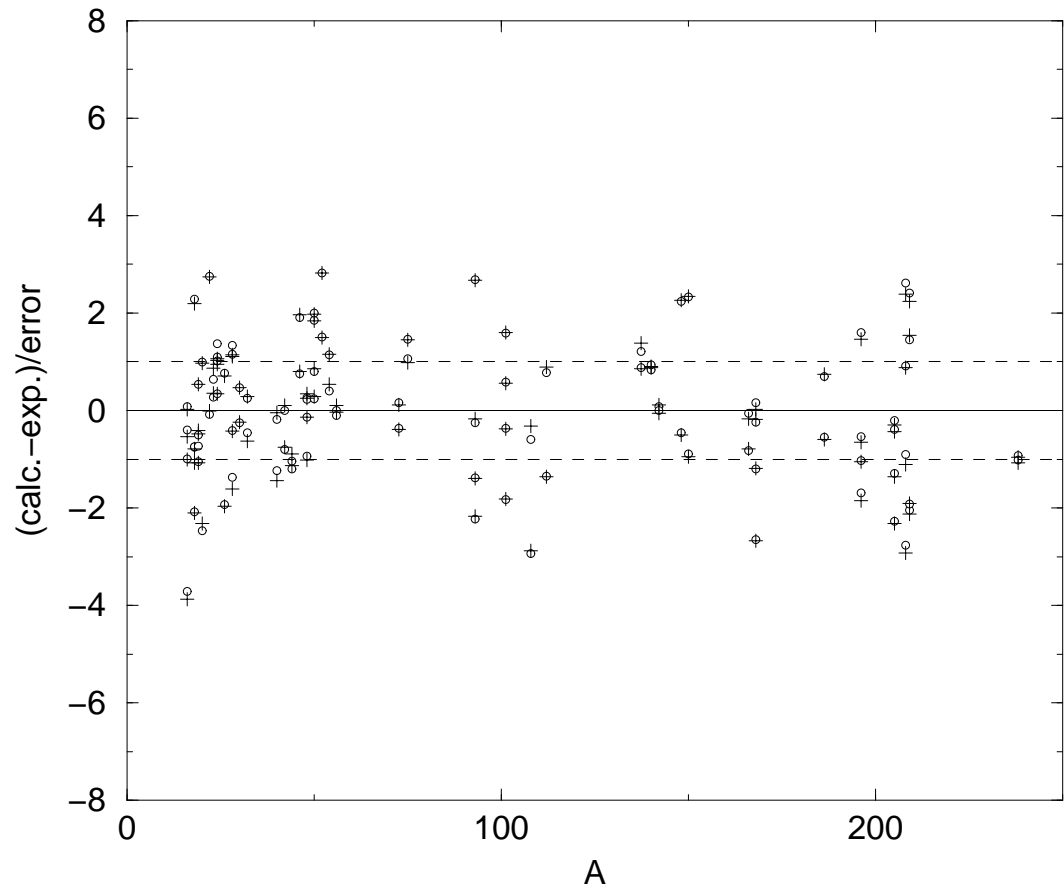


FIG. 3. Values of χ for the best fit C potential (open circles) and W potential (+ signs) using MAC densities.

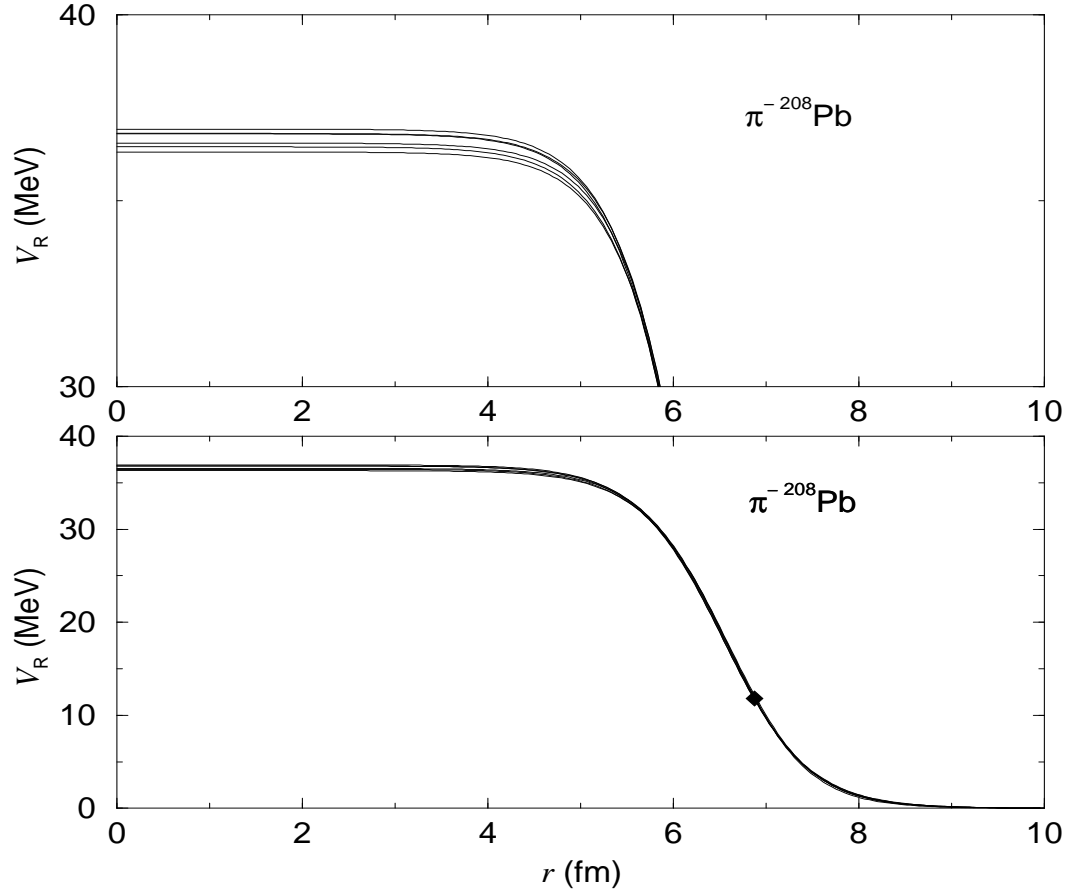


FIG. 4. The real part of the s -wave π^- ^{208}Pb potential for the six models using MAC densities. The ‘half-density’ point is indicated at 6.9 fm.

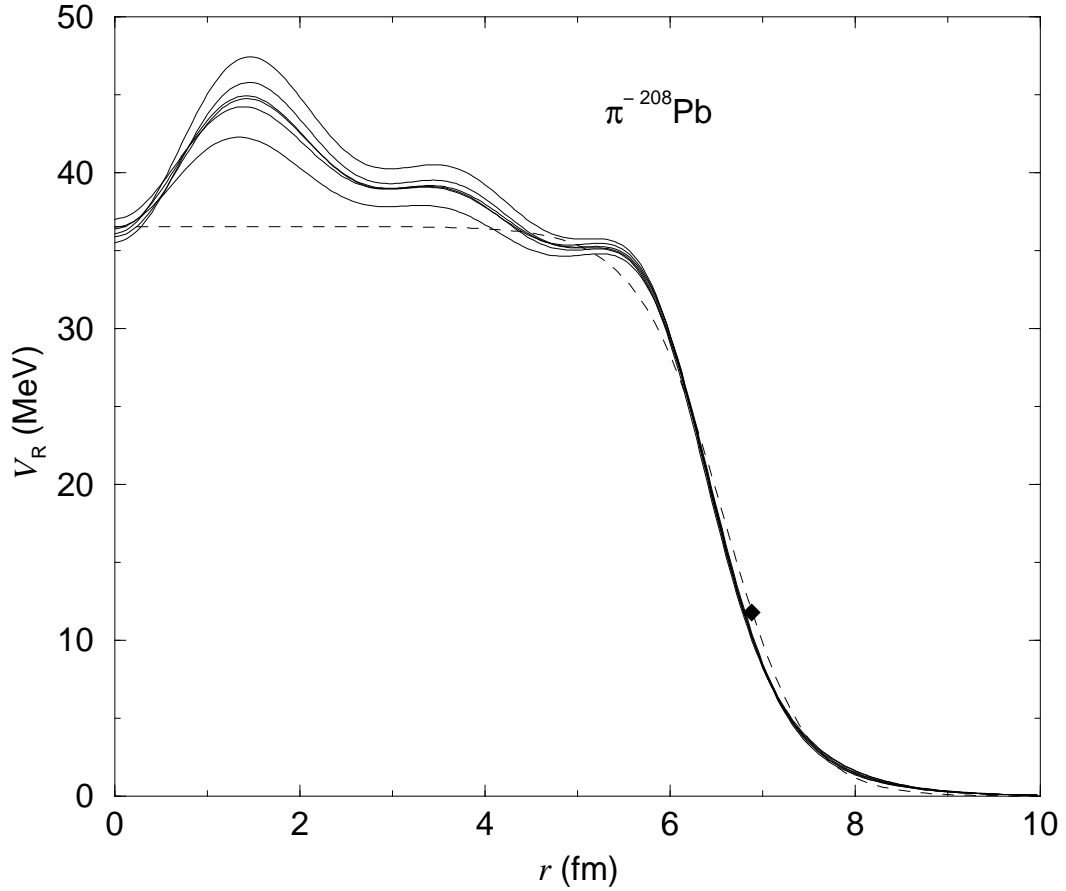


FIG. 5. The real part of the s -wave $\pi^- - {}^{208}\text{Pb}$ potential for the six models using SP densities. Also shown (dashed) is the C potential based on MAC densities. The ‘half-density’ point is indicated at 6.9 fm.